

Electronic structure analysis of the quasi-one-dimensional oxide $\text{Sr}_6\text{Co}_5\text{O}_{15}$ within the LDA+U method

A. S. Botana,^{1,2,a)} P. M. Botta,³ C. de la Calle,⁴ A. Piñero,^{1,2} V. Pardo,^{1,2} J. Botana,^{1,2} M. Pereiro,^{1,2} D. Baldomir,^{1,2} J. A. Alonso,⁴ and J. E. Arias²

¹Departamento de Física Aplicada, Universidade de Santiago de Compostela, E-15782 Campus Sur s/n, Santiago de Compostela, Spain

²Instituto de Investigaciones Tecnológicas, Universidade de Santiago de Compostela, E-15782 Campus Sur s/n, Santiago de Compostela, Spain

³Instituto de Investigaciones en Ciencia y Tecnología de Materiales (INTEMA), CONICET-UNMdP, J.B. Justo 4320 B7608FDQ, Mar del Plata, Argentina

⁴Instituto de Ciencia de Materiales de Madrid (ICMM), CSIC, Cantoblanco, 28049 Madrid, Spain.

(Presented 17 November 2010; received 24 September 2010; accepted 4 November 2010; published online 24 March 2011)

The quasi-one-dimensional cobalt oxide $\text{Sr}_6\text{Co}_5\text{O}_{15}$ is studied using first-principles electronic-structure calculations and Boltzmann transport theory. We have been able to describe the electronic structure, characterized by the structural one-dimensionality and a particular type of charge ordering, with unexpected electronic structure of the different Co atoms. The origin of the large unquenched misaligned orbital angular momenta comes out naturally from a correct description of the different crystal-field environments. The evolution with the on-site Coulomb repulsion (U) of the electronic structure and the transport properties is discussed, with a best agreement with experiment found for the smallest value of U that allows to converge the correct in-chain ferrimagnetic ground state. © 2011 American Institute of Physics. [doi:10.1063/1.3536796]

I. INTRODUCTION

To build models for correlated electron behavior in solids, many studies have focused on one-dimensional (1D) systems since they are the easiest to analyze. Among them, there has been much interest in the cobalt oxides family $A_{n+2}B'B_n\text{O}_{3n+3}$ ($A = \text{Ca, Sr, Ba}$; B' and B commonly corresponding to Co cations in a trigonal prismatic (TP) and octahedral (OH) position, respectively, and $n \in [1, \infty)$), being CoO_3 the 1D chain. The series has attracted much attention for the rather unique properties that its members exhibit such as an Ising type behavior,^{1,2} large magnetocrystalline anisotropy,² magnetization plateaus,³ magnetic phase separation,^{4,5} or enhanced thermoelectric properties.⁶ An important question is to understand the role of the electron correlations in these systems.^{1,2} For that end, we analyzed the electronic structure and transport properties of the $n=4$ member of the series, $\text{Sr}_6\text{Co}_5\text{O}_{15}$, by *ab initio* techniques. We have performed LDA+U (local density approximation plus Hubbard U) calculations to predict its properties correctly, taking into account the strongly correlated nature of the material. We have studied the evolution with U of the ground state electronic structure and the thermopower dependence with the temperature.

The electronic structure calculations were performed with the WIEN2K⁷ software based on density functional theory utilizing the augmented plane wave plus local orbitals method (APW+lo). For the calculations of the transport properties we used the BoltzTraP code⁸ based on the Boltzmann transport theory that employs the energy bands obtained using the WIEN2K software. The electronic interactions are

described within the LDA+U formalism, using different U values, taking $J=0.7$ eV for all of them. The calculations were fully converged with respect to the k -mesh and $R_{\text{mt}} K_{\text{max}}$, using a $6 \times 6 \times 6$ sampling of the full Brillouin zone for electronic structure calculations, $21 \times 21 \times 21$ for the transport properties and $R_{\text{mt}} K_{\text{max}} = 6.0$. Muffin tin radii chosen were: 1.82 a.u. for Co, 2.28 a.u. for Sr, and 1.61 a.u. for O.

II. RESULTS

$\text{Sr}_6\text{Co}_5\text{O}_{15}$ was found^{9,10} to be isostructural with $\text{Ba}_6\text{Ni}_5\text{O}_{15}$, phase reported by Campá *et al.*¹¹ The crystal structure consists of isolated, 1D infinite chains of CoO_6 polyhedra sharing faces along the c -axis that form a hexagonal lattice in the ab plane. The in-plane distance between Co chains is significantly larger than the Co-Co in-chain distance, leading to the structural quasi-one-dimensionality. The unit cell is formed by 5 Co atoms, 4 of them are situated in distorted OH and one is in a TP environment as can be seen in Fig. 1(a).

To understand how our system is influenced by the on-site Coulomb repulsion, Table I shows the magnetic moments (MM) of each cation in the structure at different U values in a range from 4.8 to 6.4 eV for the magnetic ground state solution. Smaller values of U do not stabilize a ferrimagnetic (FiM) insulating solution, underestimating the correlation effects. In such an insulating solution, Co1 is a $\text{Co}^{4+} : d^5$ cation with a MM of $\approx 1 \mu_B$. Co2 is also a $\text{Co}^{4+} : d^5$ cation and Co3 is close to a $\text{Co}^{3+} : d^6$ configuration. The details of the Co2 and Co3 MM dependency with U can be understood looking at the magnetic interactions in the chain [see Fig. 1(a)]. The coupling between Co1 and Co2 is mediated

^{a)}Electronic mail: antia.sanchez@usc.es.

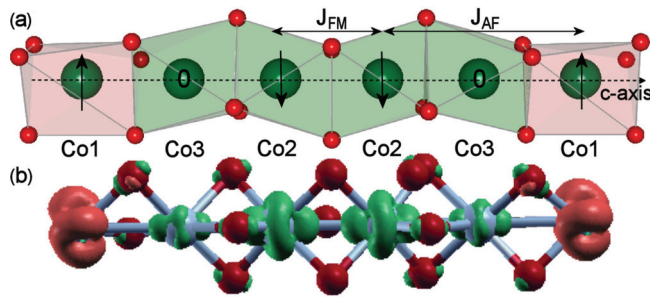


FIG. 1. (Color online) (a) Schematic picture of the structure of the CoO_3 chains in $\text{Sr}_6\text{Co}_5\text{O}_{15}$ obtained using VESTA (Ref. 13). OH environments for both Co2 and Co3 atoms as well as the TP one for Co1 are shown. We also show the ferromagnetic (FM) coupling (J_{FM}) between neighbor Co2 atoms and the antiferromagnetic (AF) one between Co2 and Co1 mediated by a nonmagnetic Co3 (J_{AF}). (b) Three-dimensional plot of the spin density in the FiM ground state, isosurface at $0.1 \text{ e}/\text{\AA}^3$ obtained using XCrysDen (Ref. 14). Spin-up density corresponds to Co1 and spin-down density corresponds to both Co2 and Co3.

by a nonmagnetic Co3. The overlap between Co3 and Co2 d-orbitals motivates a charge transfer which is higher as U decreases. An effective magnetic moment of $6.9 \mu_B$ per formula unit is found experimentally for the compound.¹² This value is larger than the spin-only one, according to the MM shown in Table I, but it is consistent with large unquenched noncollinear orbital angular momenta, as found in Ref. 12. Both Co^{3+} (Co3) atoms in the unit cell are nonmagnetic (in a low spin state, with $S = 0$) and located in OH. The Co^{4+} cations are also in a low spin state ($S = 1/2$) inside both OH (Co2) and TP (Co1) environments. The nature of the hole in the Co^{4+} d-levels depends on several factors: the different crystal field environment of each magnetic Co, the Co in-chain interaction and the crystal field distortion.

In order to interpret the electronic structure of the compound, we can consider a three-dimensional representation of the spin density. Figure 1(b) shows such representation for $U = 4.8 \text{ eV}$ (this particular choice of U will be discussed below). The spin density for Co atoms within a TP environment is clearly different from the OH one. For analyzing the spin density, we have to consider the proper coordinate system for the Co ions. The Co1 spin density can be interpreted according to the prismatic crystal field splitting, taking the z axis along the Co-chains (c -axis). The electronic structure of a $\text{Co}^{4+} : d^5$ cation in such environment is depicted in Fig. 2(a) with the hole occupying the $d_{xy}/d_{x^2-y^2}$ level in agreement with the spin density seen in Fig. 1(b) for Co1. For the OH Co atoms (Co2 and Co3), the trigonal distortion has to be taken into account² [see Fig. 2(b)]. The e_g orbitals are not affected by the trigonal distortion. The t_{2g} levels split into a higher-lying singlet a_{1g} and a lower-lying e_g^* doublet. The a_{1g} singlet spatial shape is that of a d_{z^2} orbital along the trigonal c -axis. The spin density shown

TABLE I. Projection of the spin MM inside the muffin tin spheres of Co atoms in the $\text{Sr}_6\text{Co}_5\text{O}_{15}$ ground state for different U values

Atom	MM for different U values in μ_B units				
	6.4 eV	5.8 eV	5.4 eV	5.2 eV	4.8 eV
Co1	1.24	1.17	1.12	1.09	1.05
Co2	-1.01	-0.95	-0.90	-0.87	-0.81
Co3	-0.06	-0.08	-0.10	-0.13	-0.17

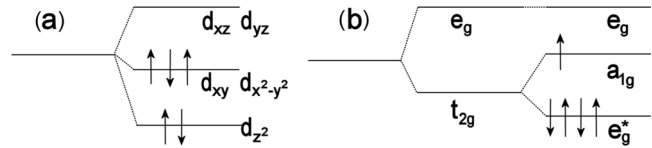


FIG. 2. Level scheme representing (a) the prismatic crystal field levels for a Co^{4+} cation and (b) the electronic structure for a Co^{4+} cation in a trigonally distorted OH environment. The splitting of the t_{2g} levels caused by this distortion can be observed.

in Fig. 1(b) for Co2 (and also for Co3 due to hybridization) corresponds to one hole in the singlet. In this case, the a_{1g} orbital is the higher-lying one since the OH $\text{Co}^{4+} : d^5$ are surrounded not only by Co^{4+} but also by Co^{3+} cations and the $\text{Co}^{4+} - \text{Co}^{3+}$ distance is smaller than the $\text{Co}^{4+} - \text{Co}^{4+}$ one. The orbital angular momenta found¹² *ab initio* come from a non-negligible contribution from the occupied e_g^* doublet.

To better understand the changes in the electronic structure of the compound as U increases, Fig. 3 shows the density of states (DOS) plots of the Co atoms in the unit cell for the two extremal U values shown in Table I ($U = 4.8 \text{ eV}$ and $U = 6.4 \text{ eV}$). The material is an insulator for this range of U values, with a d-d gap that increases from 0.5 eV to 1 eV as U does. For Co1 ($\text{Co}^{4+} : d^5$) we can see the spin split d_{xz}/d_{yz} bands (by about 1 eV for $U = 4.8 \text{ eV}$ and 1.5 eV for $U = 6.4 \text{ eV}$). For $U = 4.8 \text{ eV}$, the unoccupied $d_{xy}/d_{x^2-y^2}$ orbital for Co1 is shifted respect to the d_{xz}/d_{yz} one at about 2 eV above the Fermi level. For $U = 6.4 \text{ eV}$, such a shift does not appear and the hole is at about 2.5 eV . For Co2 ($\text{Co}^{4+} : d^5$), we can see a spin splitting of the e_g bands (by less than 1 eV for $U = 4.8 \text{ eV}$ and 1 eV for $U = 6.4 \text{ eV}$). The hole in the a_{1g} singlet of Co2 presents a double peak structure at about 1 eV above the Fermi level for the lower U value and at 1.5 eV for the higher one. For Co3, we can observe an approximate d^6 DOS plot. Due to the hybridization between Co3 and Co2 d-orbitals a double peak structure arises (at the same energy than for Co2), showing a small density of unoccupied t_{2g} states for Co3. As the overlap diminishes with increasing U values, this density is reduced for $U = 6.4 \text{ eV}$. The e_g bands for Co3 present a small spin-splitting for $U = 4.8 \text{ eV}$, negligible for the higher U value. The evolution with U of the

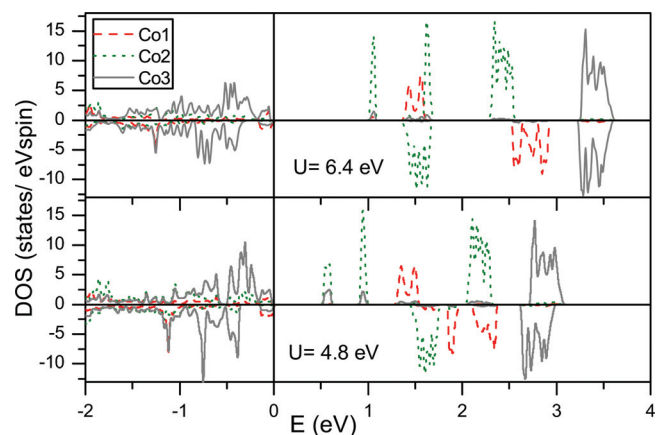


FIG. 3. (Color online) Partial spin-polarized DOS of Co1, Co2, and Co3 atoms for $U = 4.8 \text{ eV}$ and $U = 6.4 \text{ eV}$. Fermi energy is represented by the solid vertical line at zero. Upper (lower) panels show the spin-up (down) channels.

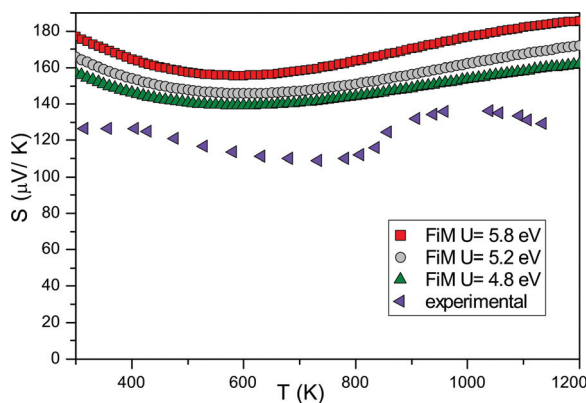


FIG. 4. (Color online) Experimental and calculated temperature dependence of the thermopower for different U values.

MM for Co_3 can be observed: its value rises from 0 as U decreases, while it lowers from $1 \mu_B$ for Co_2 . An ionic picture works in explaining the electronic structure of this insulating compound, characterized by very narrow bands. This is more evidently so for larger values of U .

We also have calculated the temperature dependence of the thermoelectric power for the FiM ground state shown in Fig. 1(a) at different U values to further analyze the system properties and its evolution with U . Using the conductivity (σ) and Seebeck coefficient (S) calculated for both spin channels, the total thermopower has been obtained according to the two-current model expression¹⁶ in the constant scattering time approximation. Figure 4 shows the data calculated at $U = 4.8, 5.2,$ and 5.8 eV together with the experimental S values taken from Ref. 15. The results for the FiM solution at $U = 4.8$ eV fit better the experimental values, both in the order of magnitude of the thermopower and also in the observed non-activated evolution with temperature. With increasing U values, the curve profile does not change but it goes to higher Seebeck values, just reflecting a rigid shift of the bands (the simplest approximation to the LDA+ U method) and an increase of the bandgap. A better agreement with the experimental Seebeck coefficient is found for the smaller U value that has been used in the past to analyze the magnetic properties of the compound;¹² this is due to the small experimental value of the bandgap.¹⁴

To summarize, we have used density-functional calculations within the LDA+ U approach and Boltzmann transport theory, to study the changes with the U value in the electronic structure and related thermoelectric power of the quasi-1D oxide $\text{Sr}_6\text{Co}_5\text{O}_{15}$. Its unit cell contains 3 magnetic Co^{4+} cations (one within a TP environment and two within an OH one) and two nonmagnetic Co^{3+} ones (octahedrally coordinated). The nature of the hole in the $\text{Co}^{4+} : d^5$ cations has been studied by

means of a three dimensional representation of the spin density and the study of the different crystal field environments. For the TP Co, due to the small trigonal distortion, an undistorted picture of the crystal field splitting is enough to understand that the hole lies in the planar degenerate $xy/x^2 - y^2$ levels. For the OH ones, the trigonal distortion has to be considered, with the hole lying in the a_{1g} singlet. The calculated Seebeck coefficient curve profile agrees with experiment but it goes to higher Seebeck values as U increases, just reflecting the rigid shift that the bands experiment due to the LDA+ U method. For the smaller U values, a better agreement with experiment is found due to the relatively small bandgap observed experimentally in this compound.

ACKNOWLEDGMENTS

The authors thank the CESGA for the computing facilities, the Ministerio de Educación y Ciencia (MEC) for the financial support through the project MAT2009-08165, the Ministerio de Ciencia e Innovación (MICINN) for the project MAT2007-60536 and the Xunta de Galicia for the project INCITE08PXIB236052PR. A.S.B. thanks MEC for a FPU grant. M.P. and J.B. thank Isabel Barreto program and Deputación da Coruña, respectively, for financial support.

- ¹H. Wu, T. Burnus, Z. Hu, C. Martin, A. Maignan, J. C. Cezar, A. Tanaka, N. B. Brookes, D. I. Khomskii, and L. H. Tjeng, *Phys. Rev. Lett.* **102**, 026404 (2009).
- ²V. Pardo, P. Blaha, R. Laskowski, D. Baldomir, J. Castro, K. Schwarz, and J. E. Arias, *Phys. Rev. B* **76**, 165120 (2007).
- ³A. Maignan C. Michel, A. C. Masset, B. Raveau, and C. Martin, *Eur. Phys. J. B.* **15**, 657 (2000).
- ⁴V. Pardo, P. Blaha, M. Iglesias, K. Schwarz, D. Baldomir, and J. E. Arias, *Phys. Rev. B* **70**, 144422 (2004).
- ⁵P. M. Botta, V. Pardo, D. Baldomir, C. de la Calle, J. A. Alonso, and J. Rivas, *Phys. Rev. B* **74**, 214415 (2006).
- ⁶T. Takami, M. Horibe, M. Itoh, and J. Cheng, *Phys. Rev. B* **82**, 085110 (2010).
- ⁷K. Schwarz and P. Blaha, *Comp. Mat. Sci.* **28**, 259 (2003).
- ⁸G. K. H. Madsen and D. J. Singh, *Comp. Phys. Commun.* **175**, 67 (2006).
- ⁹C. de la Calle, A. Aguadero, J.A. Alonso and M.T. Fernández-Díaz, *Solid State Sciences* **10**, 1924 (2008).
- ¹⁰W. T. A. Harrison, S. L. Hegwood and A. J. Jacobson, *J. Chem. Soc. Chem. Comm.* 1953 (1995).
- ¹¹J. A. Campá, E. Gutiérrez-Puebla, M. A. Monge, I. Rasines, and C. Ruíz-Valero, *J. Solid State Chem.* **108**, 230 (1994).
- ¹²A. S. Botana, P. M. Botta, C. de la Calle, A. Piñeiro, V. Pardo, D. Baldomir, and J. A. Alonso, arXiv:1009.3736v1 [cond-mat.str-el] (2010).
- ¹³K. Momma and F. Izumi, *J. Appl. Crystallogr.* **41**, 653 (2008).
- ¹⁴A. Kokalj, *J. Mol. Graphics Modell.* **17**, 176 (1999).
- ¹⁵K. Iwasaki, M. Shimada, H. Yamane, J. Takahashi, S. Kubota, T. Nagasaki, Y. Arita, J. Yuhara, Y. Nishi, and T. Matsui, *J. Alloy. Compd.* **377**, 272 (2004).
- ¹⁶H. J. Xiang and D. J. Singh, *Phys. Rev. B* **76**, 195111 (2007).